

Recurrences without closed orbits

F. Robicheaux and J. Shaw

Department of Physics, Auburn University, Auburn, Alabama 36849

(Received 30 January 1998)

The results of quantum photoabsorption calculations are presented for H, K, and Cs atoms in static electric fields. The recurrence spectra for $\langle L_z \rangle \neq 0$ show features at scaled actions an order of magnitude shorter than for any classical closed orbit of this system. Two interesting manifestations are presented, and some of the systematics of the peak strengths are explored. These features suggest that closed-orbit theory may need to be generalized to account for these effects. A heuristic formula is presented that reproduces some of these effects. [S1050-2947(98)02108-8]

PACS number(s): 32.60.+i, 03.65.Sq

The dynamics of an electron in a Coulomb potential and static fields has been extensively studied using quantum and semiclassical techniques. The quantum calculations are relatively simple to perform for low- n states, but become increasingly difficult and less accurate as n increases. Semiclassical techniques are accurate and provide insight into the dynamics at high n , but become increasingly difficult to use and less accurate for low n .

Closed-orbit theory is a semiclassical method for calculating photoabsorption cross sections. This method is based on the observation that to calculate this cross section it is only necessary to obtain the Green's function for points near the nucleus when the initial state is compact. Thus in a semiclassical approximation to the Green's function, it is only necessary to use orbits whose starting and final points are near the nucleus. The results in this paper arose from a search for generic effects that are not incorporated in the usual implementations of closed-orbit theory. Thus the effects presented in this paper do not simply indicate a discrepancy with closed-orbit theory, but seem to imply a missing mechanism which would be interesting to uncover.

In this paper, we examine the quantum dynamics of H- and alkali-metal atoms in static electric fields. If the electric field is in the z direction, the L_z operator commutes with the Hamiltonian; thus we can choose to have eigenstates of energy and L_z . For alkali-metal atoms, there are no other constants of the motion. The Coulomb plus constant field give a potential that has a saddle-point maximum at a distance $1/\sqrt{F}$ in the down-field direction. The height of this saddle is such that classical electrons with energy greater than $-2\sqrt{F}$ can leave the region near the nucleus and travel to ∞ . For energies less than this, the electron can quantum mechanically tunnel through the barrier and escape. However, the tunneling rate rapidly decreases with decreasing energy, and is negligibly small for the cases we examine in this paper.

The Hamiltonian for an electron in a Coulomb potential and a static electric field can be scaled. Our calculations are performed so that the scaled energy $\varepsilon = E/\sqrt{F}$ is a constant; E is the energy and F is the field strength. We have performed photoabsorption calculations where the squared dipole matrix elements from the initial to the final states are obtained as a function of ω where $E = \varepsilon(2\pi/\omega)^2$ and $F = (2\pi/\omega)^4$. Fourier transforming the squared dipole matrix elements with respect to ω gives the recurrence spectrum

$$R(\hat{S}) = \left| \int \rho(\omega) e^{i\hat{S}\omega} W(\omega) d\omega \right| / \int \rho(\omega) W(\omega) d\omega, \quad (1)$$

where $\rho(\omega)$ is proportional to the photoabsorption cross section divided by the laser frequency, and the weight function $W(\omega) = \exp[-(\omega - \omega_{av})^4 / \Delta\omega^4]$ limits the range of the integration. With this definition, $R(0) = 1$.

The recurrence spectrum has peaks at values of \hat{S} equal to the scaled actions for which a classical electron has a closed orbit that leaves and returns to the nucleus. The peak height is the recurrence strength. Repetitions of orbits and combinations of orbits arising from scattering from the core electrons for alkali-metal atoms also produce well-known features [1-3].

There have been two generalizations of closed-orbit theory to account for features in $R(\hat{S})$ that do not arise from closed orbits at scaled energy ε . These are the ghost orbits arising from orbits that do not exist at ε but do exist at a nearby ε [4,5]. The other generalization has been to incorporate effects from orbits that start at a node of the wave function and therefore should have zero strength in $R(\hat{S})$ (in the simple implementation of closed-orbit theory) [6].

Our present results are for $m=1$ and 2 spectra in H, K, and Cs; $m\hbar$ is the eigenvalue of the L_z operator with the z direction defined to be in the direction of the electric field. All spectra are over a fixed energy range from $-(1/800)$ to $-(1/1800)$ (i.e., $20 \leq n \leq 30$) and field strengths such that classical over-the-barrier ionization does not occur. This n range is somewhat low, but still high enough where the approximations in closed-orbit theory might be expected to work. The quantum programs used in our calculations have been described elsewhere [7].

The central idea in this paper is to stay at low enough n such that the field does not strongly mix the n manifolds. If this condition is satisfied then there will be features in $R(\hat{S})$ at very short scaled actions, where \hat{S} are integer multiples of $1/\sqrt{-2\varepsilon}$. In closed-orbit theory, these peaks would be associated with orbits that go out from the nucleus and return directly to the nucleus. If $m=0$, there are two possible orbits satisfying this condition: (1) the orbit that heads straight up the z axis and returns to the nucleus without leaving the z

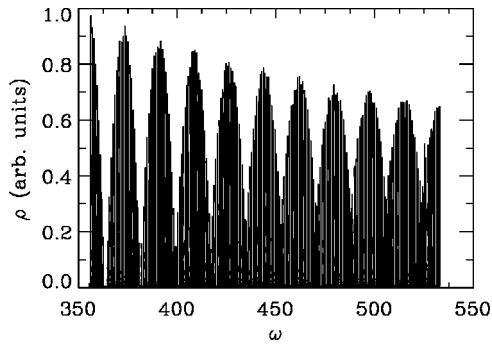


FIG. 1. H $m=1$ scaled energy spectrum for $\varepsilon=-4.0$; ρ is proportional to the photoabsorption cross section divided by the laser frequency $\omega=2\pi\sqrt{\varepsilon/E}$.

axis, and (2) the orbit that heads straight down the z axis and returns to the nucleus without leaving the z axis. If $m \neq 0$, these two orbits are not possible, because L_z is conserved and there is a repulsive $L_z^2/(x^2+y^2)$ term in the potential.

No other orbits leave from the nucleus and directly return to the nucleus. For a laser excitation to $m \neq 0$, the electron leaves the nucleus with low angular momentum. The torque from the electric field initially causes the angular momentum to increase, thus preventing the electron from returning directly to the nucleus. Eventually, the angular momentum precesses back to small values, allowing the electron to return to the nucleus with a scaled action centered at $\hat{S} \sim (-2\varepsilon)^{3/2}/3$. This action is an order of magnitude larger than that for the shortest $m=0$ closed orbit, $\hat{S} \sim 1/\sqrt{-2\varepsilon}$.

We first demonstrate the existence of peaks in the recurrence spectrum of H at actions shorter than the shortest allowed closed orbit. Because the potential is purely Coulombic, there can be no scattering from one orbit to another; any effects are the result of motion in the separable Hamiltonian of H in a static electric field. In Fig. 1, we present the squared dipole matrix element $\rho(\omega) = \sigma(\omega)/\nu(\omega)$ as a function of $\omega = 2\pi\sqrt{\varepsilon/E}$ for excitation to $m=1$ states at the scaled energy $\varepsilon = -4.0$. σ is the photoabsorption cross section, and ν is the laser frequency. This spectrum can be understood quantum mechanically as arising from the separate n manifolds of Stark states from $n=20$ to 30. The Stark states from different n manifolds only barely overlap, so probably perturbation theory could be used to calculate this spectrum.

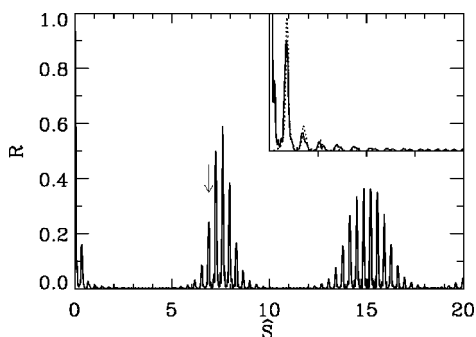


FIG. 2. H $m=1$ recurrence spectrum for $\varepsilon=-4.0$. The inset shows the regions $R \leq 0.2$ and $\hat{S} \leq 4$ by expanding both the x and y axes by a factor of 2.5. The closed-orbit result is given in the inset as a dotted line.

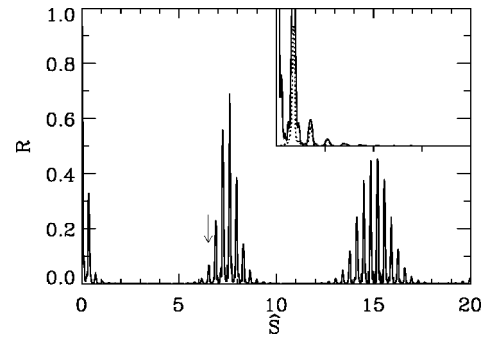


FIG. 3. Same as Fig. 2, but for $m=2$.

In Figs. 2 and 3 are the recurrence spectra for $m=1$ and for 2. These spectra are for the scaled energy of $\varepsilon = -4.0$. The arrow marks the smallest action for a closed orbit for this system, $\hat{S} = 6.89$. The inset shows the region $R \leq 0.2$ and $\hat{S} \leq 4$ by expanding both the x and y axes by a factor of 2.5. In both Figs. 2 and 3 there are peaks at actions much shorter than is possible in closed-orbit theory. In particular, the first recurrence peak is at actions $\hat{S} = 0.35$, an order of magnitude smaller than that of the shortest closed classical orbit. Note that the first recurrence peak is stronger for the $m=2$ spectrum than for the $m=1$ spectrum. When the scaled energy was varied between -3.0 and -3.5 , we found that the $m=1$ first recurrence peak was larger than that for the $m=2$ first recurrence peak, while the situation reversed for scaled energies between -3.5 and -4.0 . This is contrary to our initial expectations that the $m=1$ first recurrence peak would always be stronger because when $m=2$ the higher azimuthal angular momentum should push the orbits further from the z axis. Also, the initial angular distribution of trajectories emphasizes orbits ejected into the xy plane which are torqued the most; this should cause the electron to precess away from the low angular momentum, diminishing the recurrence strength. Some unknown dynamics controls the relative strength of these peaks.

There are features in the recurrence spectrum that appear to correspond to repetitions of this ‘‘short action orbit.’’ The recurrence strength rapidly decreases for low repetitions, but increases as the action approaches that of the allowed closed orbits. This behavior is similar to the quasiperiodic recurrence strengths of repetitions of a stable closed orbit. This similarity suggests that the effect will be understandable within an extension of closed-orbit theory.

A second effect similar to that in H can be seen in the $4s + h\nu \rightarrow m=1$ spectra of K and the $6p_{3/2}, \mu=3/2 + h\nu$

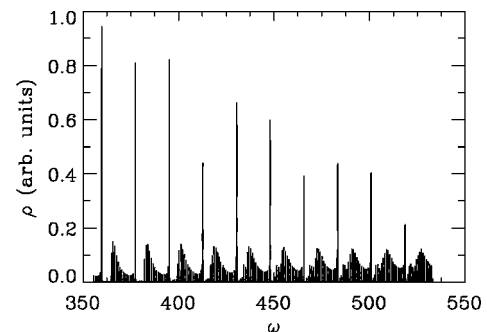
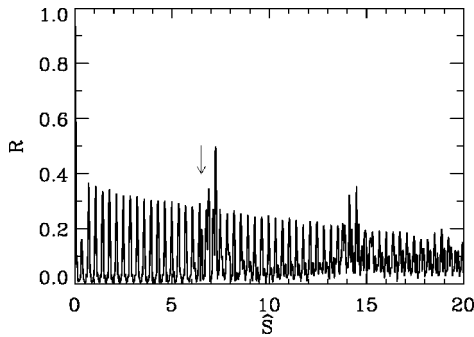


FIG. 4. Same as Fig. 1, but for K $m=1$.

FIG. 5. Same as Fig. 2, but for K $m=1$.

$\rightarrow m=2$ spectra of Cs. For these systems, the quantum defects are not negligibly small, so that scattering from the core plays a large role in the spectra. The p -wave quantum defect in K is 1.714, and the d -wave quantum defect is 0.265; the d -wave quantum defect in Cs is 2.473, and the f -wave quantum defect is 0.03. The squared dipole matrix element for the K spectrum is given in Fig. 4 for the scaled energy of $\varepsilon = -4.0$. The very tall individual peaks are the remnants of the np states that have not strongly mixed into the Stark manifold.

The recurrence spectrum for K is plotted in Fig. 5, and that for Cs in Fig. 6. These spectra are for the scaled energy of $\varepsilon = -4.0$. Again, the arrow marks the smallest action for a closed orbit for this system. There are several interesting features in the recurrence spectra. The most visible is the dominance and persistence of the short action peaks. Quantum mechanically, the explanation of this effect is fairly simple. We are at field strengths and energies such that the np states in K and the nd states in Cs do not strongly mix with the stark manifold of states. Therefore, the dominant period will be the field-free Rydberg period $\tau = 2\pi n^3$, which would be the period of an orbit that directly returns to the nucleus. The slow decay of the ‘‘repetitions’’ of this nonexistent orbit arise because the np states in K and nd states in Cs have not mixed strongly. Features strongly localized in ω will cause a slow decay in \hat{S} .

Note another interesting feature of the Cs recurrence spectrum in Fig. 6. The ‘‘repetitions’’ of the short action peak have almost completely decayed away by $\hat{S} = 5$. There are peaks in the recurrence spectrum at $6.9 \leq \hat{S} \leq 8.3$ arising from the true closed orbits of this system. After these peaks, the short action peaks reappear. Perhaps this is not too surprising, since scattering from one closed orbit into another

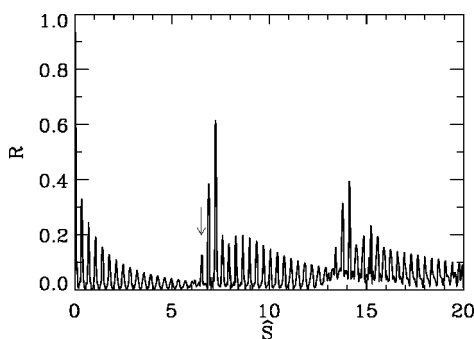
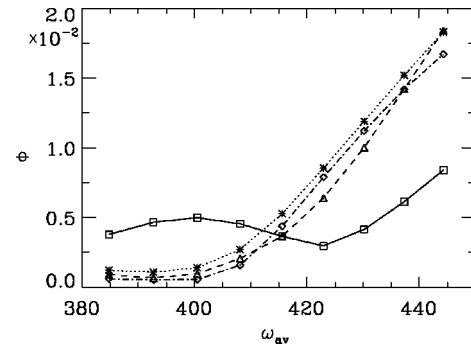
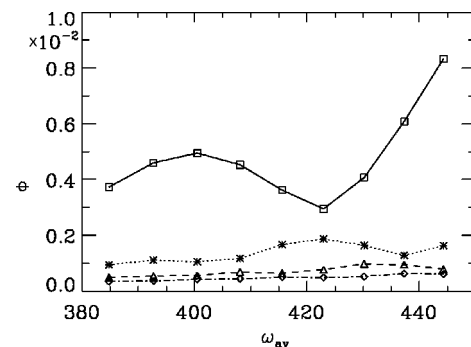
FIG. 6. Same as Fig. 2, but for Cs $m=2$.

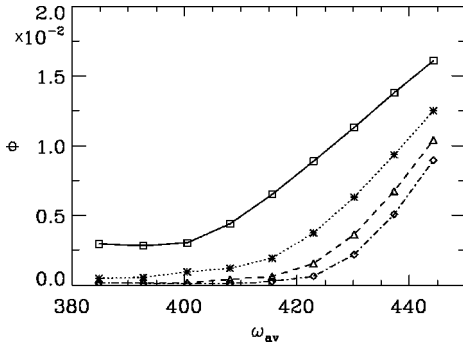
FIG. 7. K $m=1$ recurrence strength for the first four recurrence peaks: first peak—square; second peak—* ; third peak— \diamond ; fourth peak— \triangle . ϕ is defined to be the integral of R from the minimum before the n th peak to the minimum after the n th peak.

would give this effect. However, it must be remembered that the orbit being scattered into *does not exist* as a true closed orbit.

One question that should be answered is how does the strength of these recurrences depend on the scaled energy or average ω value? We have found that the behavior is not trivial, and can be quite interesting. We have defined the strength of a recurrence peak, ϕ , to be the integral of $R(\hat{S})$ from the minimum before the peak to the minimum after the peak. We have plotted this for the first four short action recurrences versus ω_{av} . Figures 7 and 8 are the $m=1$ strengths for K and H, respectively, and Figs. 9 and 10 are the $m=2$ strengths for Cs and H, respectively. In these four figures, the lowest ω_{av} point corresponds to $\varepsilon = -3$, and the highest point corresponds to $\varepsilon = -4$.

One of the features that strongly suggests that this phenomenon can be understood within an extension of closed-orbit theory is that the recurrence strength for the first peak does depend on m and ω_{av} but does not depend on the atom. Peaks 2–4 do depend on which atom is being excited, suggesting that the first peak derives from some sort of pure orbit recurrence, whereas later peaks also depend on scattering from the core electrons. Another feature is that in general the strengths of these peaks increase with ω_{av} ; this is understandable since increasing ω_{av} means the average field strength is decreasing. One interesting feature of Figs. 7 and 8 is that the strength of the first recurrence peak oscillates with increasing ω_{av} ; there is a local maximum for $\varepsilon \sim -3.25$ and a local minimum for $\varepsilon \sim -3.625$. Another interesting feature is the sharp upturn in the first recurrence

FIG. 8. Same as Fig. 7, except for H $m=1$.

FIG. 9. Same as Fig. 7, except for Cs $m=2$.

strength for Cs and H in Figs. 9 and 10; this upturn is at $\varepsilon \sim -3.25$. In Cs the 2–4 recurrence peaks have a sharp increase at the larger value $\varepsilon \sim -3.625$. On the scale used in these figures, the 2–4 recurrence peaks in both H figures show little variation, and remain small over the whole range.

The semiclassical explanation of the K and Cs spectra is not clear. Even for H the semiclassical theory is hard to imagine if we restrict the theory to closed orbits that return exactly to the origin. In the usual derivation of closed-orbit theory, the semiclassical returning wave is matched to the interior partial wave solution by defining a matching constant N , which is the ratio of the incoming semiclassical wave ψ^{sc} to the exact solution for an incoming Coulomb wave at zero energy, ψ_c , when r is large. For $m=1$, ψ_c near the z axis is

$$\psi_c = \sqrt{r-z} J_1(2\sqrt{r+z}), \quad (2)$$

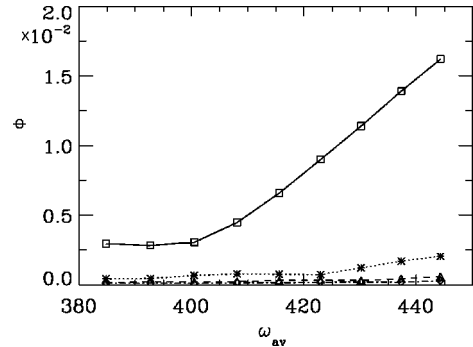
where J_1 is the Bessel function of order 1.

We constructed a semiclassical approximation for the returning wave function for $m=1$, where the node along the positive and negative z axes is incorporated into the matching constant N via the correct ψ_c , but the semiclassical wave function ψ^{sc} is computed for $m=0$ as if the classical trajectories on the axis did exist. The method used is the same as the method outlined in Ref. [6] for a nodal wave function along the direction perpendicular to the magnetic field, but now the node is assumed to be on the axis. The crucial difference between the calculations is that in the magnetic-field case [6] an orbit *does* exist in the node, while for the $m=1$ spectra in the electric field *no* orbit exists along the axis (but the features in the spectrum imply that the wave function near the axis behaves as if the orbit exists).

If we use the $m=0$ orbits and amplitudes with the nodal matching, one can show that the amplitudes are

$$C_k = \frac{16}{r_0} (E - E_i) \left| \frac{\partial \theta_i}{\partial \theta_f} \right|^2 |I(n,0,1)|^2, \quad (3)$$

where $|\partial \theta_i / \partial \theta_f|^{-1}$ is the change in the final angle as the initial angle is varied, r_0 is the matching radius, and $I(n,0,1)$ is the radial overlap of the initial atomic state with a zero energy outgoing wave with $\ell=1$. The phases of the returning waves are given by

FIG. 10. Same as Fig. 7, except for H $m=2$.

$$\Delta_k = nS_k^1 - \nu_k^n \frac{\pi}{2} + \text{sgn} \left(\frac{\partial \theta_i}{\partial \theta_f} \right) + 2\delta_1, \quad (4)$$

where S_k^1 is the action of the first return of the on-axis orbits, ν_k^n is the Maslov index, $\text{sgn}(\partial \theta_i / \partial \theta_f)$ is the sign of the angle derivative, and δ_1 is the phase shift of the $\ell=1$ partial wave arising from the core potential.

The recurrence strengths calculated for H in this approximation roughly agree with the quantum calculations (see the inset in Fig. 2). The semiclassical result was normalized to give exact agreement with the quantum result at the largest allowed peak near the scaled action of 7. The largest discrepancy in the semiclassical calculation is a 20% overestimate in the peak at $\hat{S}=0.35$. The agreement improves for the other recurrences, and we can see that there are really two fundamental actions whose repetitions give separate peaks at higher actions. These actions are 0.363 and 0.346, associated with the downhill and uphill $m=0$ orbits, respectively.

To check the validity of the semiclassical formula, we compared the closed-orbit calculations to quantum calculations done for principal quantum numbers in the ranges $30 < n < 40$ and $40 < n < 50$. By a classical scaling law (Ref. [6]) applied to Eq. (3), the isolated short action recurrences should decrease by factors of 0.5 and 0.3 as the principal quantum number is increased into these ranges. The quantum recurrences do decrease according to the classical scaling law, though there is again a noticeable discrepancy in the peak height for the shortest action for $30 < n < 40$. This discrepancy is strongly reduced for $40 < n < 50$. This first peak is sensitive to the relative amplitudes and phases of the ‘‘uphill’’ and ‘‘downhill’’ returning waves, more so than any of the other short action recurrences. These deviations may reflect shortcomings in the approximations made deriving Eqs. (3) and (4).

A formula similar to Eq. (3) can be derived for $m=2$ excitation. Comparisons between the semiclassical and quantum calculation in Fig. 3 show overall agreement in recurrence amplitude and scaling behavior. The first peak at $\hat{S}=0.35$ is now underestimated by 50%, but the agreement improves rapidly for the higher action recurrences. For both the $m=1$ and $m=2$ formulas, the agreement is best for the weaker recurrences and the highest principal quantum numbers. Both describe the general behavior of the peaks, but the $m=1$ formula is much better at reproducing the quantum results.

To extend these heuristic formulas to atoms heavier than H (for instance the $m=1$ K and $m=2$ Cs presented in this paper), requires calculating the p and d components of the core scattered wave produced by the returning nodal wave. Since the core scattering is incorporated into closed-orbit theory by a perturbative expansion of the Green's function, it currently works best for weak scattering of low partial waves. Strong scattering in K and Cs in the p and d waves is required to reproduce the effects seen in the quantum spectra. The current semiclassical theory does not work for these cases. This topic is under investigation.

Although we obtain decent agreement with the quantum H results, we stress that these are heuristic equations, and we do not have a justification for using the nonexistent orbits in the semiclassical theory. It appears that a justification for this

procedure must come from outside the usual implementation of closed-orbit theory. It may be that the closed-orbit theory needs to incorporate orbits that do not start and end with radial orbits near the nucleus. Or maybe the semiclassical Green's function needs to include orbits that are not quite classical. Or maybe there is an end point contribution to the semiclassical Green's function in addition to the stationary phase points that are usually included. None of these suggestions may be correct; however, the results presented in this paper suggest that closed-orbit theory is missing a mechanism for describing some aspects of scaled energy spectra. We expect similar effects for other types of static fields.

This work was supported by the NSF and the U.S. Department of Energy with Auburn University.

-
- [1] D. Delande, K. T. Taylor, M. H. Halley, T. van der Veldt, W. Vassen, and W. Hogervorst, *J. Phys. B* **27**, 2771 (1994).
- [2] M. Courtney, H. Jiao, N. Spellmeyer, and D. Kleppner, *Phys. Rev. Lett.* **73**, 1340 (1994); M. Courtney, N. Spellmeyer, H. Jiao, and D. Kleppner, *Phys. Rev. A* **51**, 3604 (1995).
- [3] P. A. Dando, T. S. Monteiro, D. Delande, and K. T. Taylor, *Phys. Rev. Lett.* **74**, 1099 (1995); P. A. Dando, T. S. Monteiro, D. Delande, and K. T. Taylor, *Phys. Rev. A* **54**, 127 (1996).
- [4] M. K us, F. Haake, and D. Delande, *Phys. Rev. Lett.* **71**, 2167 (1993).
- [5] J. Main, G. Wiebusch, K. H. Welge, J. Shaw, and J. B. Delos, *Phys. Rev. A* **49**, 847 (1994).
- [6] J. Shaw, J. Delos, M. Courtney, and D. Kleppner, *Phys. Rev. A* **52**, 3695 (1995).
- [7] F. Robicheaux and J. Shaw, *Phys. Rev. A* **56**, 278 (1997).